The Thesis Committee for Jiawei He
Certifies that this is the approved version of the following thesis:

Fabrication of Hierarchical Gold Nanoblades with High Surface Enhanced Raman Scattering Activity

APPROVED BY
SUPERVISING COMMITTEE:

Supervisor:

Donglei Fan

Hu Tao

Fabrication of Hierarchical Gold Nanoblades with High Surface Enhanced Raman Scattering Activity

by

Jiawei He

Thesis

Presented to the Faculty of the Graduate School of

The University of Texas at Austin

in Partial Fulfillment

of the Requirements

for the Degree of

Master of Science in Engineering

The University of Texas at Austin

December 2017

Acknowledgements

I would like to express my sincere appreciation to all those who provided help for me in working on this thesis. First of all, I would like to deeply thank my advisor, Dr. Donglei Fan. Her excellent ideas and patient guidance have helped me substantially in my research. Her unique perspectives of chemistry and materials science, have led me to understand my research and experiments much more deeply. I also would like to appreciate Dr. Hu Tao for his precious time and suggestions as a reader of my thesis.

My fellow labmates have provided helpful guidance to my research as well. Chao Liu, Jianhe Guo and Weigu Li, have helped me immensely, through answering my questions, discussion of my experiment results, and teaching me the operation of experimental setups. Their patience and knowledge have motivated me in pursuing my research. Particularly, Chao Liu's guidance in synthesizing silver nanocapsules and Raman testing has been indispensable to my experiments.

Lastly, I would like to also thank my parents in providing support for me during these few years of my study in my master degree. Your love and support make me a better person.

Abstract

Fabrication of Hierarchical Gold Nanoblades with High Surface Enhanced Raman Scattering Activity

Jiawei He, M.S.E.

The University of Texas at Austin, 2017

Supervisor: Donglei Fan

To obtain high sensitivity, efficiency, reproducibility and specificity, has been the goal in biochemical detection. Surface enhanced Raman scattering (SERS), which utilizes localized surface plasmon resonance (LSPR) of noble metals to significantly enhance Raman signals of molecules, is one of the most promising techniques for bio-sensing. Silver has been the dominant substrates for SERS due to its ultrahigh sensitivity. Comparing to silver, gold has its advantages in better bio-compatibility, less toxicity, and more tunable surface plasmon resonance (SPR) properties for potential photothermal applications in cancer treatment. Developing spiky gold nanostructures with sharp tips and dense junctions is the key to making its SERS performance comparable to silver.

In this study, the synthesis of Au nanoblades for SERS activity with high sensitivity has been explored. By utilizing the galvanic replacement reaction between chloroauric acid ($HAuCl_4$) and Ag nanocapsules with 3,4-dihydroxyphenylalanine (DOPA) as surfactant and reducing agent, a new spiky structure of Au nanoblades coated on Ag nanocapsules

was successfully synthesized. The concentration of DOPA and reaction time can significantly affect the number and morphology of Au blades. The lengths of Au nanoblades can vary from 20 nm to 100 nm under different reaction conditions. The SEM and EDS results have demonstrated the mechanism of the growth of Au nanoblades and the role of DOPA. The formation of AgCl during galvanic reaction between $HAuCl_4$ and Ag nanoparticles can promote non-epitaxial growth of Au on the AgCl precipitates. DOPA serves as a reducing agent to reduce $HAuCl_4$ to Au and a capping agent to favor the growth of sharp tips. Raman test results showed that the Au nanoblades detected Raman spectra of Nile blue with a concentration as low as 10^{-10} M. The high sensitivity and detection limit can be attributed to the dense sharp tips and small junctions as hotspots along the whole surface of the nanocapsules, which is comparable to the state-of-the-art Ag SERS substrates.

Table of Contents

List of Tables

List of Figures

Introduction

More than 40 years have passed since Fleischmann *et al.*, firstly discovered that electrochemically roughened silver (Ag) electrodes can significantly enhance the Raman scattering spectrum of pyridine molecules [1]. Since then, countless efforts have been put in the research of surface enhanced Raman scattering (SERS). By utilizing localized surface plasmon resonance (LSPR) of noble metal nanostructures to substantially enhance Raman signals of molecules, SERS is one of the most promising techniques for bio-molecule sensing with high sensitivity and efficiency. At confined positions of nanostructures, such as the junctions of adjacent nanoparticles and the tips of nanostars, electric (E) fields are greatly enhanced. These locations are called hotspots [2]. SERS has quadruple dependence on the localized E-field, which makes the enhancement in the localized E-field a dominating factor to SERS [4]. Therefore, developing substrates with plentiful hotspots is the key to improve SERS performance. Different types of SERS substrates have been developed in the previous research, including roughened metal surfaces, nanogaps, sharp nanostructures and core-shell nanostructures. Different methods can be applied for the fabrication of these substrates, such as chemical etching, electrochemical deposition, lithography patterning, bio-assisted assembly [5].

Although Ag generally has better performance in SERS enhancement than gold (Au), Au has its unique advantages in better bio-compatibility, less toxicity, and broader tunable surface plasmon resonance (SPR) band for other applications such as near-infrared photothermal effect [6]. Compared to the smooth Au nanoparticles with a similar size,

spiky nanostructures, such as nanoflowers and multi-pods, present a more significant enhancement in SERS performance, due to the numerous hotspots in every individual nanoparticle [7]. Different approaches can be utilized to generate complex Au spiky structures, including one-plot synthesis, seed-mediated method, galvanic replacement reaction and lithography.

In this study, we utilized Ag nanocapsules reported in the previous research [8] to study the synthesis of Au nanoblades with sharp tips via a galvanic reaction between chloroauric acid ($HAuCl_4$) and Ag nanoparticles. Different reaction conditions were examined, to tune and optimize the number and morphology of Au nanoblades. After obtaining the optimal nanoblades sample, Raman testing was conducted to compare the SERS performance of this spiky structure to the state-of-the-art Ag substrates.

Chapter 1: Literature Review

1.1 Surface Enhanced Raman Scattering

1.1.1 Background

The goal in biochemical detection is to obtain high sensitivity, efficiency, specificity and reproducibility. Surface enhanced Raman scattering (SERS), which utilizes localized surface plasmon resonance (LSPR) to significantly enhance Raman signals of molecules, is one of the most promising techniques for sensing. Electrons in conduction bands can oscillate collectively in noble metal nanostructures, which can substantially enhance electric (E) fields in specific nanoscale locations. These confined nanoscale positions are called hotspots, such as the junctions of adjacent nanoparticles and the tips of nanostars [2]. Near hotspots, Raman scattering spectra of molecules are significantly increased with $|E|^4$ dependence [3]. SERS has been widely applied in analytical chemistry, single molecule sensing, environmental monitoring and biomedical detection.

However, the practical applications of SERS are still facing a few obstacles. It is difficult to develop nanostructures as substrates that can provide enough uniform hotspots for SERS enhancement. Identifying the hotspots of a SERS substrate takes a great amount of time and efforts. The substrates need to be reproducible and have relatively long life-time for repeat usage. Lastly, abundant bio-chemicals in practical environment make it challenging to determine the SERS signals of the desired species [5].

1.1.2 Mechanisms

SERS performance can be affected by two major factors: electromagnetic

enhancement induced by the plasmonic resonance of noble metal nanoparticles [9] and chemical enhancement induced by the charge-transfer of the noble metal particles and analytes [10]. When electromagnetic waves interact with a metal nanoparticle, the electrons in conduction bands of a metal nanoparticle oscillate collectively, which induces enhanced localized E-field. SERS has quadruple dependence on the localized E-field: $EF \approx \frac{|E(\omega_L)|^4}{|E_0|^4}$, where *EF* is the enhancement factor, E_0 is the external field and the localized *E* field has a resonant angular velocity ω_L [11]. Therefore, the enhancement of the localized E-field is a dominating factor to SERS and the most effective approach to improve SERS sensitivity.

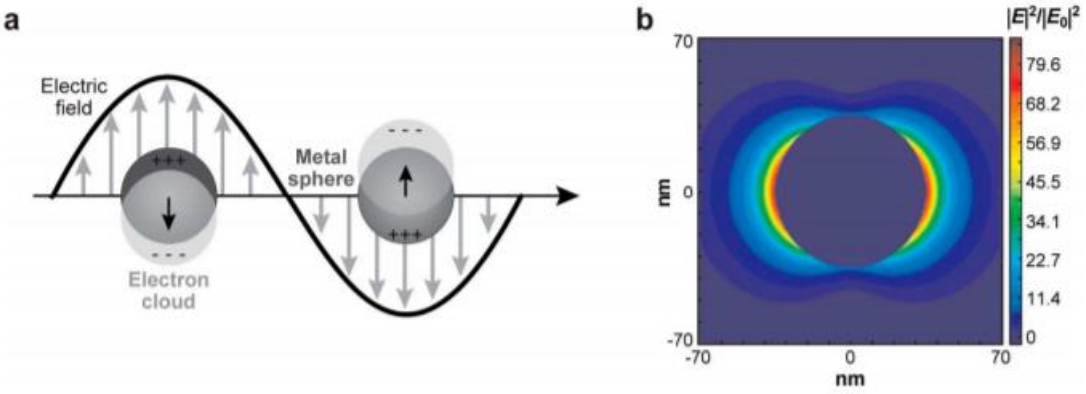

Figure 1.1: (a) Schematic of localized surface plasmon resonance (LSPR); (b) Extinction coefficient of a Ag nanoparticle of 35 nm in vacuum. [12]

1.1.3 Typical SERS Substrates

1. 1. 3. 1 Roughened Metal Surfaces

Roughened silver electrodes are the first-studied SERS substrates in history [10]. Roughened metal surfaces provide plentiful hotspots for SERS application. Templated electrochemical deposition of Ag or Au can produce thin films with roughened surfaces on top of the electrodes [13].

Chemical etching is also a typical approach for generating roughened surface. Caob, *et al.*, showed that Fe electrode with chemical etching by H_2SO_4 and KCl can lead to roughened surface and improved performance in SERS performance [14]. Leonid, *et al.*, demonstrated that roughed star-fruit shaped Au nanorods have significantly better SERS enhancement comparing to smooth Au nanorods [15]. However, these roughened metal surfaces generally can not provide effective number of hotspots and therefore do not have significant SERS performance in actual applications.

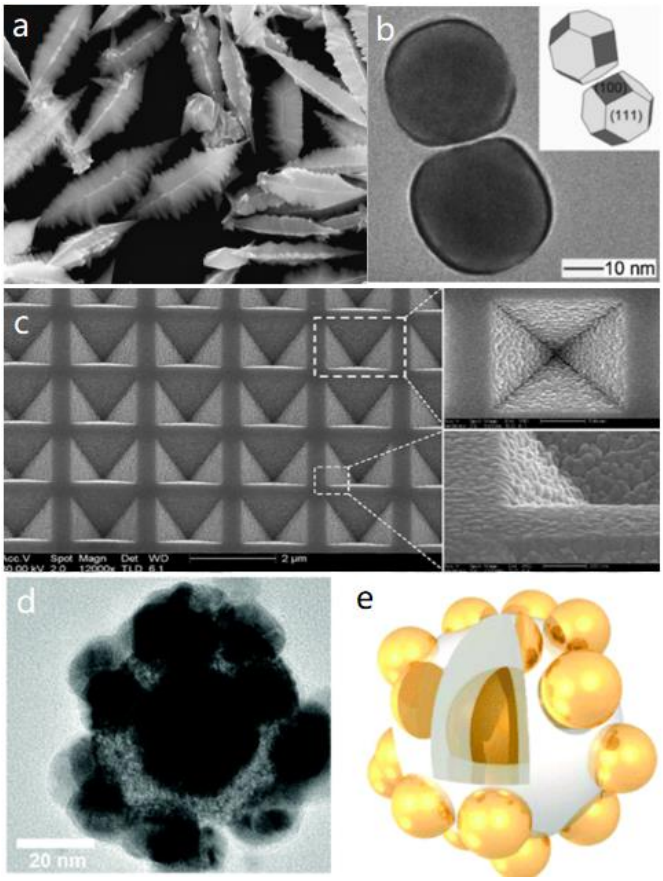

Figure 1.2: Typical substrates for SERS: (a) starfruit gold nanowires with roughened surface [15]; (b) silver nanosphere dimers [20]; (c) arrays of pyramidal wells with roughened gold structure [23]; (d, e) Au/Pt/Au nanoraspberry [25]

1. 1. 3. 2 Nanogaps

Nanogaps with a size less than 2 nm between nanoparticles are effective hotspots for SERS [16]. By controlling the aggregations nanoparticles, nanogaps can be formed, such as dimers, trimers and clusters. The formation of dimers and trimers typically involve linker molecules for binding interactions between monomers. Feldheim, *et al.*, have demonstrated that multivalent thiol-linkers can be utilized to form small clusters of Au nanoparticles [17]. Chen, *et al.*, have shown that thiol-terminated hydrophobic ligands can functionalize the surface of Au nanoparticles and then polymers can be utilized to encapsulate them to form Au dimers [18].

Bio-assisted fabrication is an effective approach for forming dimers and trimers. DNA origami is frequently used as a scaffold to assemble Au nanoparticles on specific sites [19].

However, the formation of dimers and trimers usually involve complicated surface functionalization. The biological or organic linkers may prevent the analytes from approaching the hotspots, which limits the SERS applications of these structures [20].

1. 1. 3. 3 Sharp Nanostructures

Nanostructures with sharp tips or branches can provide effective hotspots for SERS. Lithography is a frequently used technique for generating arrays of periodic sharp nanostructures. Typically, polymer nanopyramids templates with sharp tips are prepared in advance. Then, a thin layer of Ag or Au is coated on top of the templates through sputtering.

Nanoimprinting lithography can be applied to producing sharp polymer templates [21]. This template-assisted method can produce sharp nanostructures with high efficiency. However, tuning the morphology and size of sharp tips may be challenging.

Chemical synthesis is another approach for fabricating sharp nanostructures. By selecting appropriate surfactants and controlling reaction conditions such as temperature, anisotropic growth of nanoparticles can be favored and leads to formation of sharp structures [22].

1.1.3.4 Core-shell Nanostructures

Core-shell nanostructures generate small junctions between the core and shell, which can be applied as SERS substrates. Typically, the core and shell are composed of Au or Ag, and a thin layer of silica or polymers is placed between to separate the two components. This thin layer helps settle the relative locations of the two components and therefore the gap size [24]. Xie, *et al.*, have synthesized a core/shell Au/Pt/Au nanoraspberry structure for in-situ detection of Pt-catalyzed reactions utilizing SERS enhancement [25]. Core-shell structures can also be applied to integrating two distinct functionalities into a single particle, such as combining plasmonic and magnetic properties for more complicated applications [26].

1.2 GOLD SPIKY NANOSTRUCTURES

Although Ag generally has better performance in SERS enhancement than Au, Au has its unique advantages in better bio-compatibility, less toxicity, and broader tunable SPR

band for other applications such as near-infrared photothermal effect [6]. Recent researches have shown that Au branched nanostructures such as dendrites, nanostars and multi-pods, which have plentiful dense hotspots in the individual nanoparticles, can substantially enhance local E-field [7]. Compared to the smooth Au nanoparticles with a similar size, these spiky nanostructures present a more significant enhancement in SERS performance.

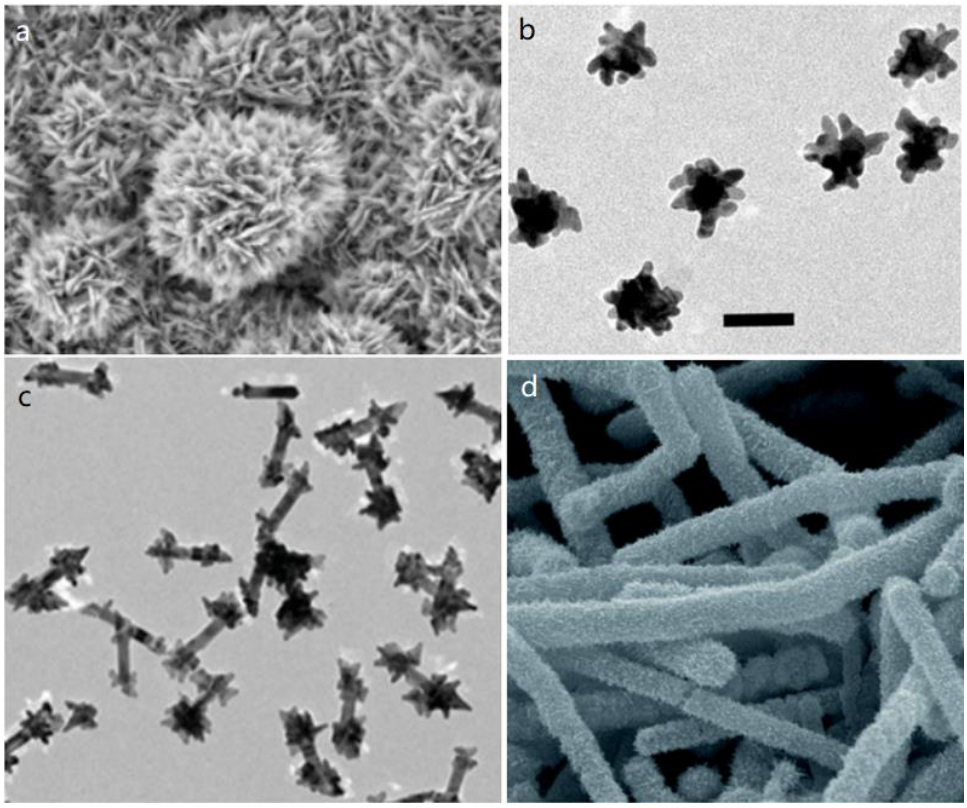

Figure 1.3: Au spiky nanostructures: (a) Au nanoflowers [27]; (b) Au nanostars [28]; (c) Au spiky nanodumbbells [29]; (d) Au caterpillar-like nanotubes [30]

1.2.1 Synthetic Methods

Various methods have been developed for synthesizing Au spiky nanostructures.

In the next sections of this chapter, I will summarize various represented synthesis techniques, such as one-pot synthesis, seed-mediated method, galvanic replacement reaction and top down lithography [31].

1. 2. 1. 1 One-pot Synthesis

One-pot synthesis is the most convenient approach for synthesizing Au spiky structures. Au precursors, reducing agent and capping agent are placed in one reaction container. By selecting appropriate surfactants and controlling reaction conditions such as reaction time and temperature, anisotropic growth of Au nanoparticles can be favored and leads to formation of spiky structures. Ascorbic acid, sodium borohydride ($NaBH_4$), sodium citrate and hydroxylamine can be employed as reducing agents to reduce $HAuCl_4$ to Au. Capping agents with long chains are critical to the non-epitaxial growth of Au spiky structures [6].

1. 2. 1. 2 Seed-mediated Method

For this method, typically gold seed nanoparticles (1–3 nm) are prepared beforehand. They can be synthesized by using $NaBH_4$ to reduce $HAuCl_4$ with adding sodium citrate which serves as a surfactant. Next, a growth solution containing $HAuCl_4$ and reducing agents are added to the seeds. Hydroxylamine, sodium citrate, and ascorbic acid are the typical reducing agents used in this step [32]. Surfactants are necessary in controlling the shapes of Au nanostructures. Hexadecyltrimethylammonium bromide (CTAB) and tetradodecylammonium bromide (TCAB) are frequently used capping agents

in the synthesis of Au branched structures. The trimethylammonium group of CTAB can attach to specific crystallographic facets of the Au seeds selectively, and the other side of the chain molecules of CTAB can form a bilayer structure via van der Waals forces, which is crucial to the formation of Au branched structures [33].

1. 2. 1. 3 Galvanic Replacement Reaction

Galvanic replacement reaction provides an effective way to synthesize noble metal nanoparticles with porous structures and hollow interiors along the surface. For this method, a metal template, such as Ag and Cu, is applied as a sacrificial template for galvanic replacement of Au. Xia *et al.* utilized Ag nanocubes as templates to synthesize Au nanocages. The standard reduction potential of the Ag^+/Ag pair is lower than $AuCl_4^-/Au$, which provides the driving force for the galvanic replacement reaction [34].

$$3Ag(s) + AuCl_4^-(aq) \Rightarrow Au(s) + 3Ag^+(aq) + 4Cl^-(aq) \quad (1.1)$$

The replacement reaction of Ag and $HAuCl_4$ can form small holes and hollow structures on specific sites, due to the Kirkendall effect [50]. AgCl is generated during the reaction, which has a low solubility in H_2O and deposits onto the whole surface of Ag nanoparticles. The formation of AgCl precipitates is critical to promoting the growth of Au non-epitaxially on the AgCl precipitates. With more $HAuCl_4$ solution is added and reduced to Au by reducing agents, the heterogeneous growth of Au will be dominant. This eventually leads to the formation of Au hollow or spiky structures [35-37].

1. 2. 1. 4 Lithography

Lithography is a broadly used technique in making periodic substrates over a large area, such as arrays of nanotips and nanocones. Typical lithographical techniques include electron beam lithography (EBL), photolithography, nanosphere lithography (NSL) and nanoimprint lithography (NIL) [38,51]. To apply lithography methods for fabricating Au spiky structures, typically polymer nanopyramids templates with sharp tips are prepared in advance. Then, a thin layer of Au is coated on top of the templates through sputtering [39]. Wu *et al.*, develped the fabrication of polymer cones with high density and dense sharp tips, through 3D NIL with silicon cones. The SERS substrates using these sharp tips coated with Au layers showed a sub-zeptomole detection limit for 1,2-bis(4-pyridyl)-ethylene (BPE) [40].

.

1.2.2 State-of-the-Art Au Spiky Nanostructures

Different types of Au spiky nanostructures have been successfully synthesized, including Au nanostars [27], Au nanoflowers [28], Au spiky nanodumbbells [29] and Au caterpillar-like nanotubes [30]. They usually have roughened surfaces and different numbers of tips and branches

1. 2. 2. 1 Au Nanostars

Au nanostar is one of the spiky structures that are firstly synthesized successfully in research [41]. Star-shaped Au nanoparticles can be synthesized via a one-pot colloid chemical synthetic approach with CTAB. The limitation of this method is that it can only produce star-shape multipods with only several nanotips. Highly branched gold nanostars

with more tips are usually obtained via a seed-mediated method [42-44].

1. 2. 2. 2 Au Nanoflowers

Compared to Au nanostars typically with only a few tips, nanoflowers generally have more petal-shaped tips, which are more useful in SERS application. Nanoflowers can be obtained through a galvanic replacement reaction. Pradhan *et al.*, have reported polystyrene bead supported Cu nanoparticles can react with $HAuCl_4$ to form Au nanoflowers with dense petal-shaped tips at 90℃ [27]. The galvanic exchange rate and strong polarization effect are crucial to the formation of the branches on the nanoflowers [45-46].

1. 2. 2. 3 Au Spiky Nanodumbbells

Au spiky nanodumbbells comprise a Au nanorod with multiple spikes at both ends. It combines two unique properties of Au nanorods and Au nanostars. The synthesis of this nanostructures is based on the seed-mediated growth approach, by reduction reaction of $HAuCl_4$ on as-prepared Au nanorods. Poly(N-vinylpyrrolidone) (PVP) and N,N-dimethylformamide (DMF) are employed for assisting the growth of Au nanostars on both ends of Au nanorods [29].

The growth of spikes at the Au nanorods can impact the longitudinal and transverse resonance modes differently. A significant redshift is usually induced for the longitudinal resonance mode, and the transverse mode only redshifts slightly and becomes broader in wavelengths. These two distinct absorption peaks provide potential application in dual functionalities [29, 47-49].

1. 2. 2. 4 Au Caterpillar-like Nanotubes

Au caterpillar-like nanotubes provide sharp tips and hollow interior along the whole surface of the nanotubes. Yang *et al.*, have reported the synthesis of caterpillar-like roughened Au/Ag nanotubes, by using Ag nanowires as a sacrificial template. 3,4-dihydroxyphenylalanine (DOPA) was crucial to the growth, serving as reducing agent and surfactant. The galvanic reaction between the $HAuCl_4$ and Ag nanowires produced the hollow interior along the nanotubes. The layer of hollow structure served as a platform for further growth of the spiky tips on the surface [30]. The dense spiky tips and hollow interior provide a significant amount of hotspots for SERS enhancement.

1.3 Summary of Literature Review

Surface enhanced Raman scattering (SERS), which utilizes localized surface plasmon resonance (LSPR) to significantly enhance Raman signals of molecules, is one of the most promising techniques for bio-molecule sensing with high sensitivity and efficiency. Since SERS has quadruple dependence on the localized E-field and the enhancement in E-field is generally the most significant factor to SERS, developing substrates with plentiful hotspots is the key to improve SERS performance. Various types of SERS substrates have developed in the previous research, including roughened metal surfaces, nanogaps, sharp nanostructures and core-shell nanostructures. Different methods can be applied for the fabrication of these substrates, such as chemical etching, electrochemical deposition, lithography patterning, bio-assisted assembly.

Although Ag generally has better performance in SERS enhancement than Au, Au

has its unique advantages. Compared to the smooth Au nanoparticles with a similar size, spiky nanostructures, such as nanoflowers and nanostars, present a more significant enhancement in SERS performance, due to the numerous hotspots in every individual nanoparticle. Different approaches can be utilized to generate complex Au spiky structures, including one-plot synthesis, seed-mediated method, galvanic replacement reaction and lithography. These synthetic methods provide a guidance for me to design a feasible approach to synthesize Au nanoblades.

Chapter 2: Experimental Setup and Characterization

In this chapter, I will introduce the experimental setup and procedure for synthesizing Ag nanocapsules and Au nanoblades. Characterization techniques including SEM, EDS, Raman spectroscopy will also be demonstrated.

2.1 Experimental Set-up

2.1.1 Fabrication of Nanocapsules

Ag nanocapsules were fabricated with a method reported in the previous research [8]. Au nanowires were synthesized by electrochemical deposition into a nanoporous anodic aluminum oxide (AAO) template. A 500nm thick Cu layer was deposited on one side of the template via E-beam evaporation. The Cu layer sealed the nanopores of the template and served as a cathode. A platinum (Pt) wire and Ag/AgCl electrode were employed as an anode and a reference electrode, respectively. Before the deposition of Au segment, a segment of sacrificial Cu and Ni nanowires was deposited in the AAO template, to enhance the contact and uniformity of the interface between Au nanowires and the Cu layer. The electrolyte for depositing Au nanowires was cyanide based solution (434 HS RTU, Technic Inc.). The total number of electrons passing through the device controlled the lengths of different segments. The electrical charges and voltages for each segment are shown in Table 2.1

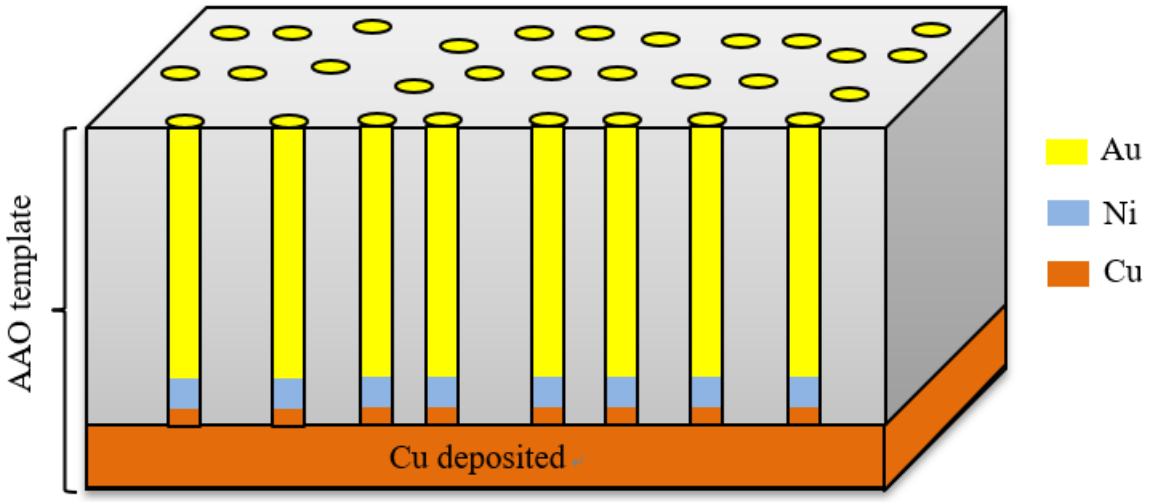

Figure 2.1: Schematic of Au nanowires deposited in the AAO template

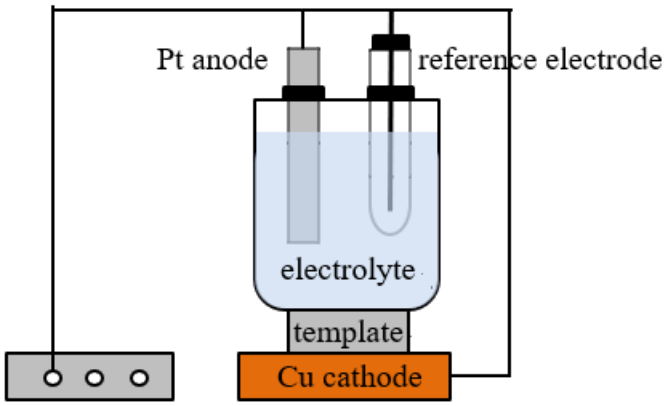

Figure 2.2: Schematic of a three-electrode electrochemical deposition device

Materials / Conditions	Cu nanowire	Ni nanowire	Au nanowire
Charge (C)	-6 C	-0.142C	-4.73C
Applied Potential (Ag/AgCl)(V)	-0.20 V	-0.80 V	-0.92 V

Table 2.1: Electrodeposition conditions for Au nanowires

After the electrochemical deposition, the sacrificial Cu/Ni segments and Cu layer on the AAO template were chemically etched. An aqueous solution of NaOH (2 M) was used to dissolve the AAO template to release the Au nanowires in the nanopores. Nanowires were rinsed twice in ethanol and deionized (D.I.) water and redispersed in D.I. water.

Afterwards, the hydrolysis reaction of tetraethyl orthosilicate (TEOS) was utilized to synthesize a thin silica layer on the entire surface of Au nanowires. 0.8 mL of TEOS was mixed with 3 mL of ethanol, 0.2 mL of ammonia and 1.8 mL of D. I. water. The mixture was sonicated for 1 hour. The silica layer was used to support the growth of Ag nanoparticles (NPs). For the final step, Ag NPs were synthesized on the whole surface of SiO2 layer by the reduction reaction of $AgNO_3$ to Ag. The as-prepared Au@SiO2 nanowires were mixed with freshly dissolved $AgNO_3$ (500 µL, 0.06 M) and ammonia (250 µL, 0.12 M), and kept under stirring for 1 hour. After they were fully mixed, polyvinylpyrrolidone (PVP, 25 µM in ethanol, 10 mL, Mw=40000 g/mol) was added to

promote the growth of Ag nanoparticles. After 7 hours of reaction at 70 ℃, dense Ag nanodots were synthesized and covered the whole surface of Au@SiO2 nanocapsules.

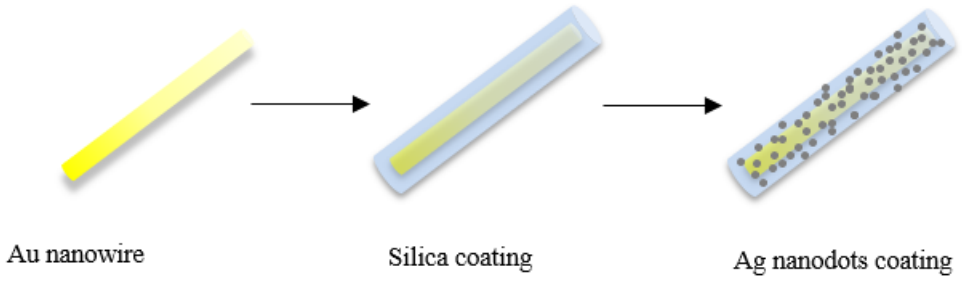

Figure 2.3: Schematic of the fabrication of Ag nanocapsules

2.1.2 Synthesis of Au Nanoblades

The Au nanoblades were synthesized via a galvanic reaction of $HAuCl_4$ and Ag NPs, combined with redox reaction of 3,4-dihydroxyphenylalanine (DOPA) and $HAuCl_4$, based on a method described in previous research [30]. Ag nanocapsules were used as the sacrificial template and DOPA was utilized as both the reducing agent and surfactant to favor the growth of Au spiky nanoblades.

100 µL of as-prepared aqueous solution of Ag nanocapsules was combined with 1.35 mL of H_2O under stirring at a speed of 500 rpm. Then 150 µL of $HAuCl_4$ (50 mM) was added immediately. After 30 seconds of reaction, 500 µL of DOPA (10 mM) solution was quickly added into the reaction solution. After 10 min, the final product of Au nanoblades was washed with D.I. water three times and redispersed in ethanol.

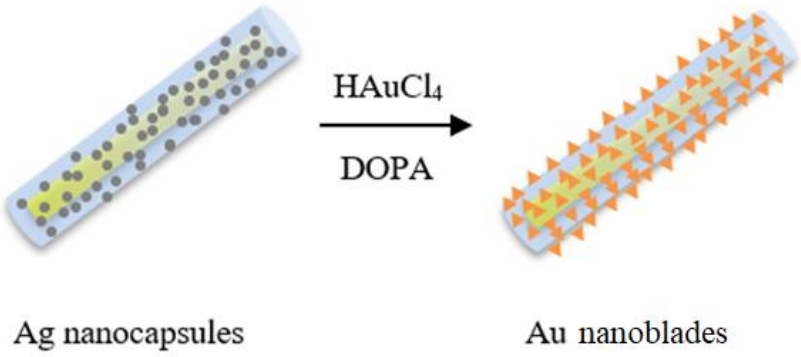

Figure 2.4: Schematic of growth of Au nanoblades from Ag nanocapsules

2.1.3 Optimization of Au Nanoblades

The morphology and number of Au nanoblades can be tuned and optimized by changing the concentrations of DOPA (the ratio of $HAuCl_4$ and DOPA) and reaction time. We applied 5 mM, 10 mM, 15 mM and 20 mM of DOPA in different synthetic batches. Reaction time was examined for 2.5 min, 5 min, 7.5 min and 10 min, respectively.

2.2 CHARACTERIZATION

2.2.1 SEM/EDS

The morphology of the Ag nanocapsules and Au nanoblades were characterized with Scanning Electron Microscope (SEM – FEI Quanta 650 ESEM). Energy Dispersive Spectroscopy (EDS) was also utilized to examine the composition of the nanoblades.

2.2.2 Raman Spectroscopy

We measured the Raman scattering signals of Nile blue solutions with different

concentrations (100 nM, 10 nM, 1 nM, 0.5 nM, 0.1 nM). The nanoblades were mixed with 20 μL of Nile blue solution for 10 mins incubation before measurements. A 633 nm Helium-Neon laser (random polarized, Research Electro-Optics, Inc.) was utilized as the excitation source to measure Raman scattering spectra. The resulting signals were filtered by a 633 nm edge filter and analyzed by a high sensitive spectrometer (Acton 2500, Princeton Instruments, Inc).

Chapter 3: Results and Discussion

3.1 SEM Images of Ag Nanocapsules And Au Nanoblades

As shown in Figure 3.1, Au nanowires with lengths of 9 ± 0.2 μm are covered with a SiO_2 layer of 160 nm thickness. Dense small Ag nanodots are obtained on the whole surface. The size of Ag NPs and hot spot junctions are 27 ± 5 nm and 1.9 ± 0.4 nm. The size of NPs and junctions can be tuned by the ratio of $AgNO_3$ and ammonia.

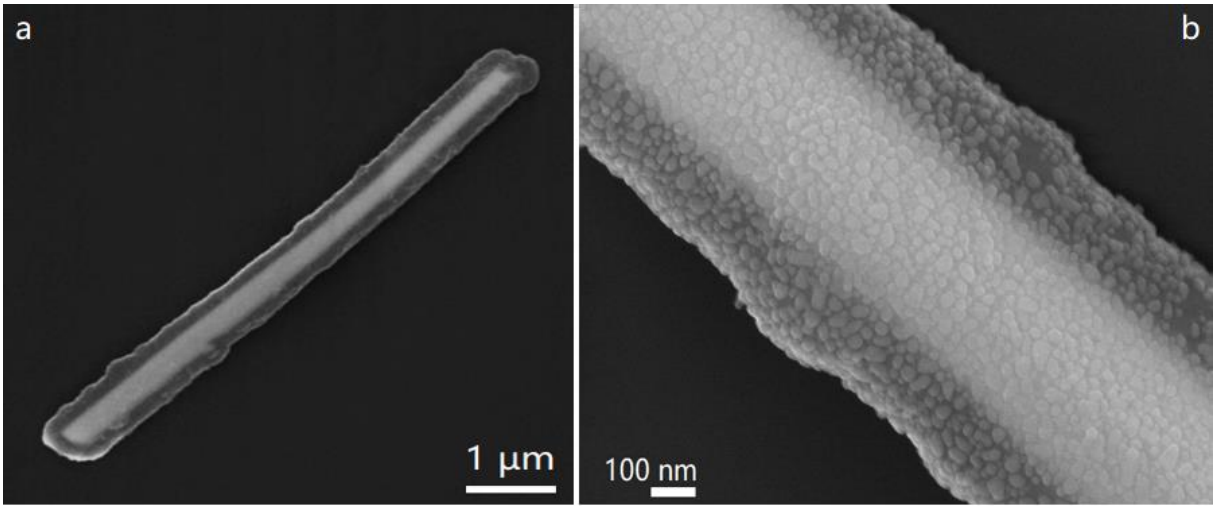

Figure 3.1: SEM images of Ag nanocapsules (a,b)

The as-prepared Ag nanocapsules were used as a sacrificial template to grow Au nanoblades on top of the Ag NPs. As shown in Figure 3.2, dense sharp blades with length of 40 ± 10 nm are synthesized on the whole surface of nanocapsules. Along with nanoblades, dense small particles with diameter of 5 nm grow on larger chunks with diameter of 90 ± 10 nm. These sharp blades and dense small particles provide plentiful hotspots for SERS application.

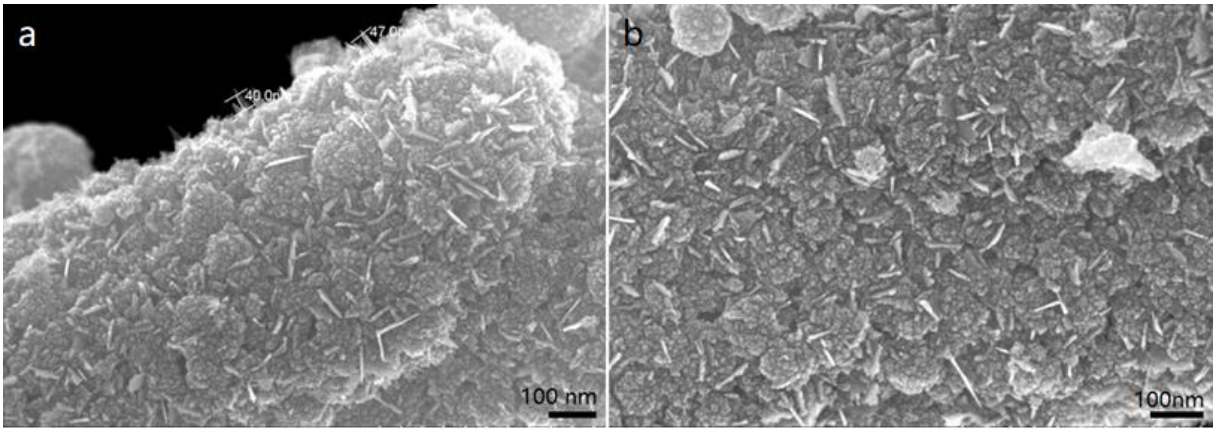

Figure 3.2: SEM images of Au nanoblades grown on Ag nanocapsules (a,b)

Energy dispersive spectroscopy (EDS) spectra were taken at the nanoblades. The spectra indicate that the nanoblades are mainly composed of Au (Figure 3.3). This result demonstrates that Ag nanocapsules can be used as sacrificial templates for replacement reaction with $HAuCl_4$ to promote the growth of complex Au spiky nanostructures. By selecting appropriate surfactant and capping agent, the size and morphology of the nanostructure obtained from galvanic replacement can be controlled. In this work, DOPA was selected as the reducing agent and capping agent, which favors the anisotropic growth of Au sharp blades.

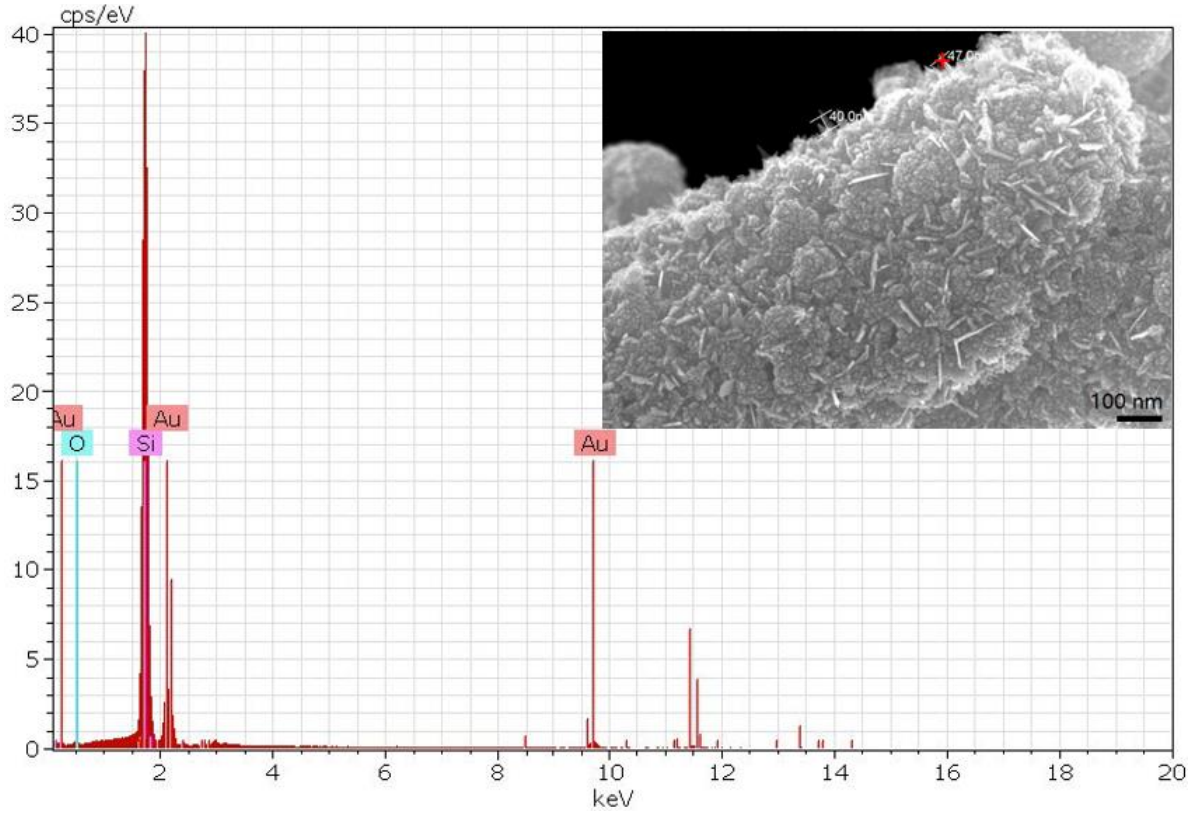

Figure 3.3: Energy dispersive spectroscopy (EDS) spectrum of nanoblades

3.2 Optimization of Au Nanoblades

In this section, different reaction conditions for the growth of Au nanoblades were studied, to tune and optimize the size and morphology of the nanoblades.

As shown in Figure 3.4, the number and size of nanoblades increase as the concentration of DOPA increases. When the concentration of DOPA is 5mM, only a few nanoblades grow on the surface of the nanocapsules. Instead, the surface is covered with dense particles with diameter of 5 nm. The junctions between the particles are mostly around 1.5 ± 0.5 nm. As the concentration of DOPA increases from 5 mM to 20 mM, the lengths of the nanoblades can vary from 20 nm to 100 nm.

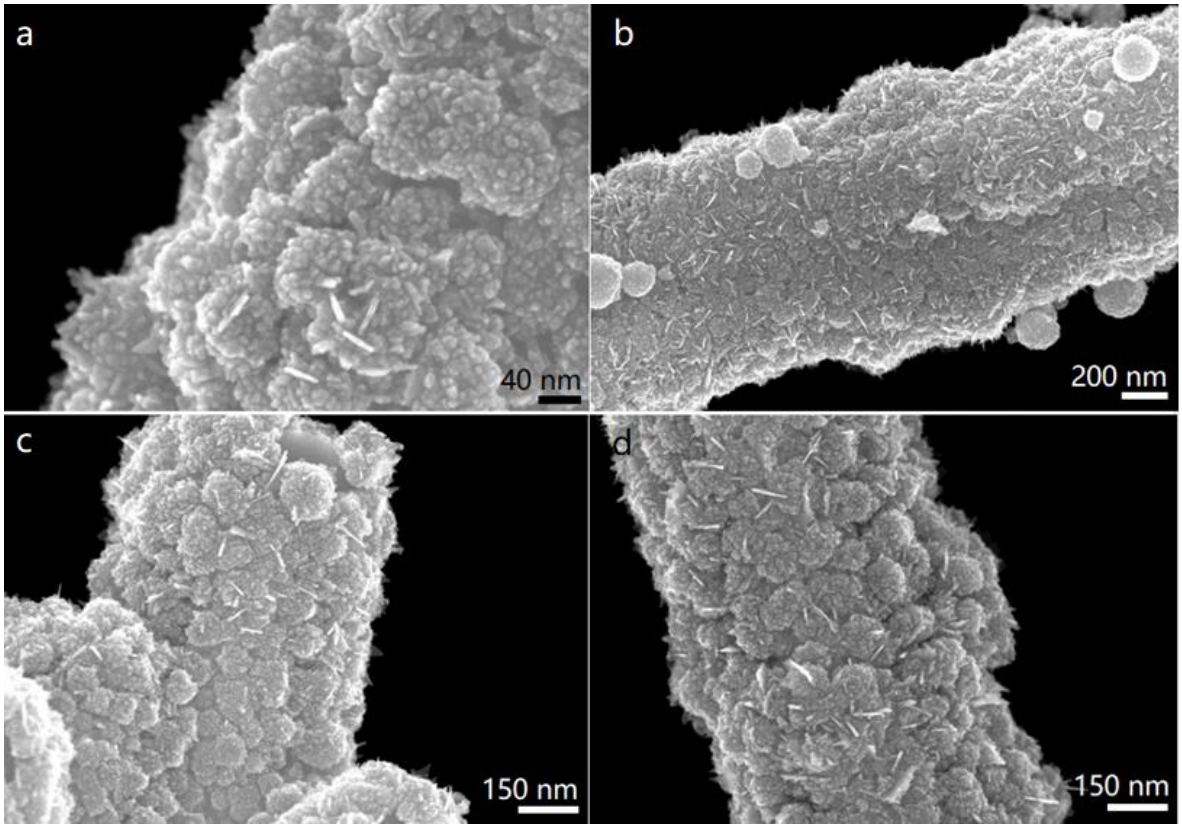

Figure 3.4: SEM images of nanoblades under different concentration of DOPA: (a) 5, (b) 10, (c) 15, (d) 20 mM

Reaction time also has a significant effect on the morphology of nanoblades. As the reaction time increases, the junctions between larger particles decrease and particles become denser. Significant blades start to grow on the surface of the particles after 5 min. More nanoblades appear and the length of nanoblades increases as the reaction proceeds. The length of nanoblades can vary from 20 nm to 80 nm. EDS spectra taken at 2.5 min demonstrate that the particles are composed of Au and Ag, which indicates the galvanic reaction between $HAuCl_4$ and Ag nanodots is not complete yet.

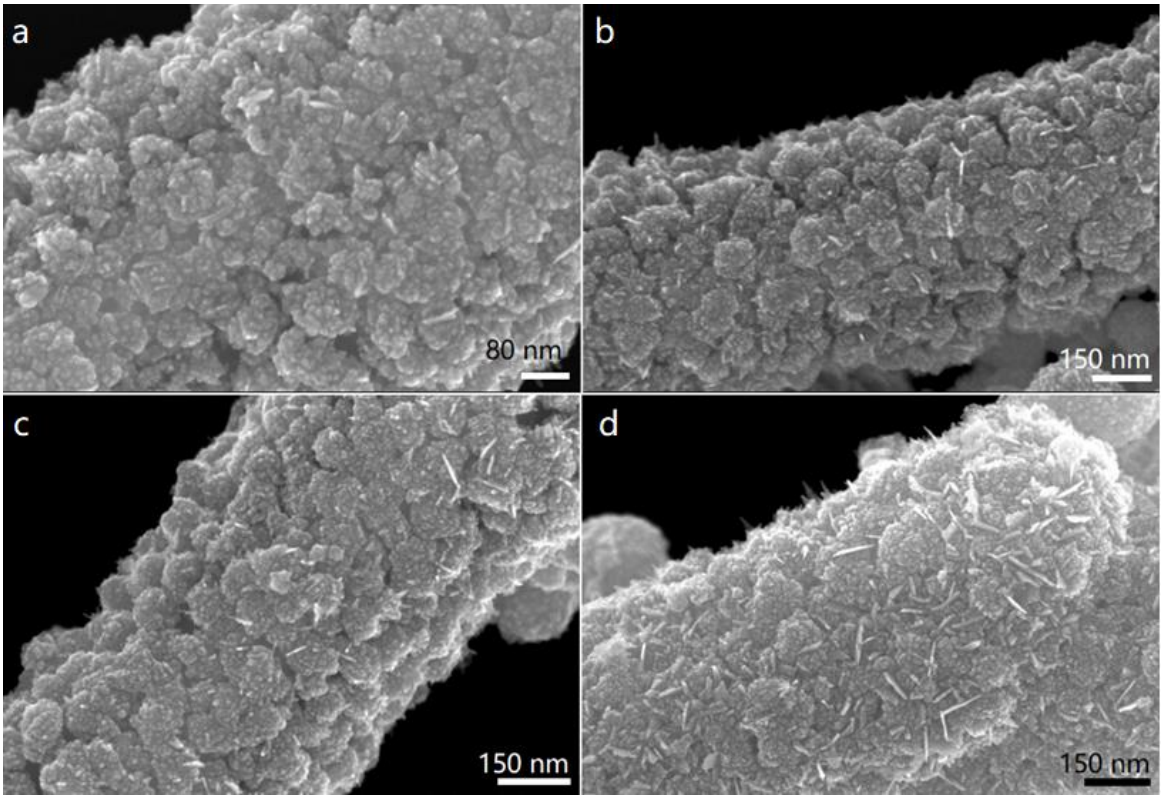

Figure 3.5: SEM images of Au nanoblades under different reaction time: (a) 2.5, (b) 5, (c) 7.5, (d) 10 min with DOPA concentration of 10 mM.

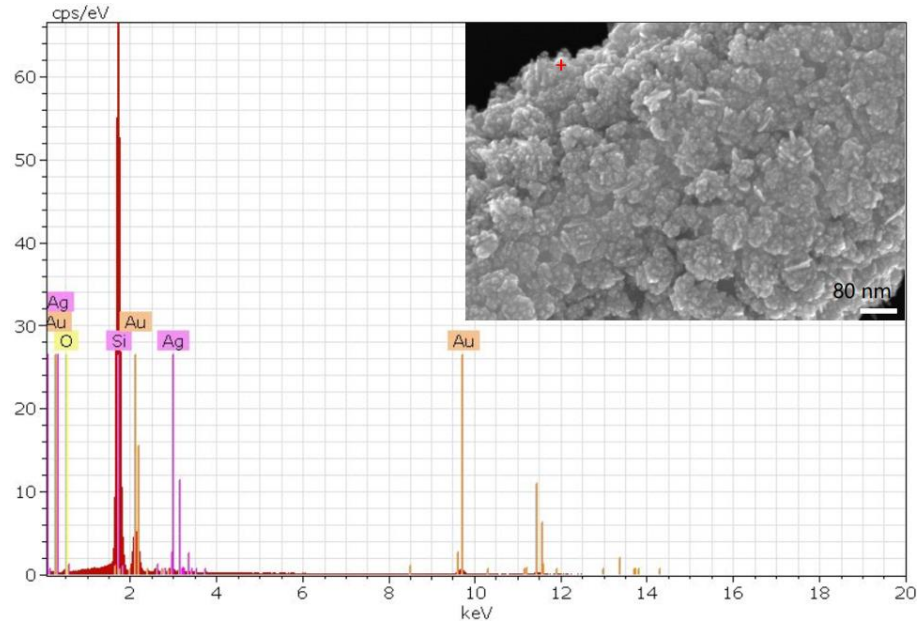

Figure 3.6: Energy dispersive spectroscopy (EDS) spectrum of nanoblades at 2.5 min

The results indicate the mechanism of the growth of Au nanoblades and the role of DOPA. Similar to the mechanism described in previous research [30], at the early stage of growth, the dominant reaction is the galvanic reaction between $HAuCl_4$ and Ag nanocapsules. The reaction generates AgCl precipitates, which have a low solubility in H_2O and deposit on top of Ag NPs. The formation of AgCl can promote the growth of Au non-epitaxially on the AgCl precipitates. After adding DOPA into the reaction, the residual $HAuCl_4$ continues to be reduced to Au by DOPA. DOPA serves as a capping agent to favor the growth of Ag spiky nanoblades. The heterogeneous growth of Au induces the formation of spiky blades on the surface of the nanocapsules. Therefore, the ratio of $HAuCl_4$ and DOPA is critical to the number and length of the nanoblades obtained. The sample with 10 mM DOPA added and 10 min reaction time has the most dense and uniform nanoblades and small junctions, therefore it is chosen for the characterization of SERS sensitivity. It is also notable that a few spiky Au nanospheres exist in the solution, which may be the growth of Au on the AgCl precipitates in the solution.

3.3 RAMAN TESTING RESULTS

In this section, the SERS sensitivity of the Au nanoblades was characterized. Nile blue was used as a testing molecule and its characteristic Raman peak at 595 cm^{-1} was examined. The test results showed that the Au nanoblades detected Raman spectra of Nile blue with a concentration as low as 10^{-10} M (100 pM). The detection limit is comparable to the state-of-the-art Ag SERS substrates. The high sensitivity can be attributed to the dense sharp tips and small junctions as hotspots along the whole surface of the nanocapsules.

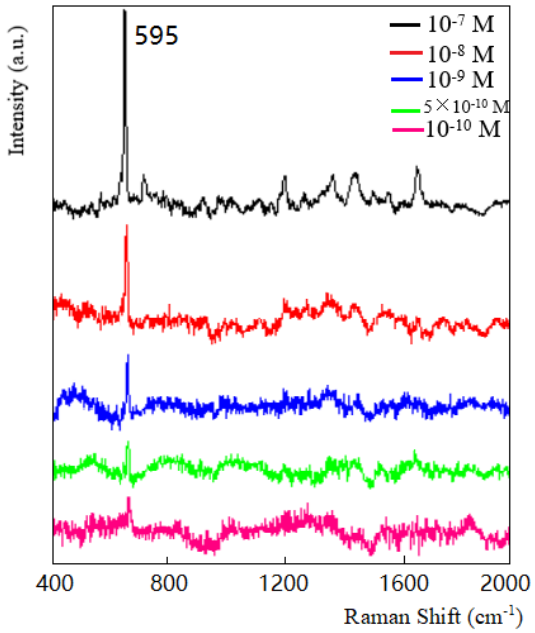

Figure 3.7: SERS spectra of Nile blue from 0.1 nM to 100 nM

3.4 Summary And Discussion

With a method reported in the previous literature, Ag nanocapsules were fabricated under a continuous process of electrochemical deposition of Au nanowires, hydrolysis of TEOS to form a SiO_2 layer, and coating of dense Ag NPs. Using Ag NPs as sacrificial templates, galvanic replacement reaction can promote the growth of Au nanoblades. DOPA was added to continue reducing $HAuCl_4$ to Au blades and served as a capping agent at the same time. SEM images showed that dense sharp nanoblades with length of 40 ± 10 nm and dense small particles with diameter of 5 ± 2 nm were formed on the surface of the original nanocapsules. EDX spectra indicated the nanoblades were mainly composed of Au.

To tune and optimize the morphology and size of the Au nanoblades, different reaction conditions were examined. The number and length of nanoblades increased as the

concentration of DOPA increased. The optimal concentration of DOPA appeared to be 10 mM, as the nanocapsules had the most dense and uniform nanoblades and small junctions under this condition. When the concentration of DOPA is 5mM, only a few nanoblades grew on the surface of the nanocapsules. Instead, the surface was mostly covered with dense particles with diameter of 5 nm. The lengths of the nanoblades varied from 20 nm to 100 nm, as the concentration of DOPA increased from 5 mM to 20 mM. Reaction time also had a significant effect on the morphology of nanoblades. The size of junctions between larger particles decreased and particles became denser as the reaction proceeded. EDS spectra taken at early stage demonstrated that the particles were composed of Au and Ag, which indicated the galvanic reaction between $HAuCl_4$ and Ag nanocapsules was not complete yet. The lengths of nanoblades varied from 20 nm to 80 nm, as the reaction time increased from 2.5 min to 10 min.

The galvanic reaction between $HAuCl_4$ and Ag NPs generates AgCl deposited on the surface of Ag NPs. The formation of AgCl can induce the non-epitaxial growth of Au on the AgCl sites. DOPA serves as a reducing agent to reduce $HAuCl_4$ to Au and a capping agent to favor the growth of sharp blades. The ratio between $HAuCl_4$ and DOPA is critical to the number and morphology of the nanoblades obtained.

Raman test results showed that the Au nanoblades detected Raman spectra of Nile blue with a concentration as low as 10^{-10} M (100 pM). The high sensitivity and detection limit can be attributed to the dense sharp tips of nanoblades and small junctions as hotspots along the whole surface of the nanocapsules, which is comparable to the state-of-the-art Ag SERS substrates.

Chapter 4: Conclusion

In this research, I have studied the synthesis of gold nanoblades for surface enhanced Raman scattering activity with high sensitivity. I have reviewed the mechanism of SERS and typical SERS substrates developed in the previous research. I have also summarized the synthetic methods for Au spiky nanostructures and state-of-the-art Au sharp nanostructures. In this project, by using the galvanic reaction between $HAuCl_4$ and Ag nanocapsules with DOPA as surfactant, I successfully synthesized a new spiky structure of Au nanoblades coated on Ag nanocapsules. Moreover, I have studied how reaction conditions can tune and optimize the size and morphology of Au nanoblades. The concentration of DOPA and reaction time can significantly affect the number and length of Au tips. The SEM and EDS results have demonstrated the mechanism of the growth of Au nanoblades and the role of DOPA. The galvanic reaction between $HAuCl_4$ and Ag NPs generates AgCl deposited on the surface of Ag NPs. The formation of AgCl can promote the growth of Au non-epitaxially on the AgCl precipitates. DOPA serves as a reducing agent to reduce $HAuCl_4$ to Au and a capping agent to favor the growth of nanoblades. Raman test results showed that the Au nanoblades detected Raman spectra of Nile blue with a concentration as low as 10^{-10} M, which is comparable to the state-of-the-art Ag SERS substrates.

Comparing to Ag substrates, Au has its advantages in better bio-compatibility, less toxicity, and more tunable SPR properties for potential photothermal applications in cancer treatment. The results of this study suggest the feasibility of building bi-functional

nanosensors for SERS and photothermal applications using Au nanoblades.

Bibliography

[1] Fleischmann, M., Hendra, P. J., & McQuillan, A. J. (1974). Raman spectra of pyridine adsorbed at a silver electrode. *Chemical Physics Letters*, 26(2), 163-166.

[2] Bailo, E., & Deckert, V. (2008). Tip-enhanced Raman scattering. *Chemical Society Reviews*, 37(5), 921-930.

[3] Camden, J. P., Dieringer, J. A., Wang, Y., Masiello, D. J., Marks, L. D., Schatz, G. C., & Van Duyne, R. P. (2008). Probing the structure of single-molecule surface-enhanced Raman scattering hot spots. *Journal of the American Chemical Society*, 130(38), 12616-12617.

[4] Xu, X., Li, H., Hasan, D., Ruoff, R. S., Wang, A. X., & Fan, D. L. (2013). Near-field enhanced plasmonic-magnetic bifunctional nanotubes for single cell bioanalysis. *Advanced Functional Materials*, 23(35), 4332-4338.

[5] Xu, X., Kim, K., Liu, C., & Fan, D. (2015). Fabrication and robotization of ultrasensitive plasmonic nanosensors for molecule detection with Raman scattering. *Sensors*, 15(5), 10422-10451.

[6] Hu, M., Chen, J., Li, Z. Y., Au, L., Hartland, G. V., Li, X., ... & Xia, Y. (2006). Gold nanostructures: engineering their plasmonic properties for biomedical applications. *Chemical Society Reviews*, 35(11), 1084-1094.

[7] Jiang, Y., Wu, X. J., Li, Q., Li, J., & Xu, D. (2011). Facile synthesis of gold nanoflowers with high surface-enhanced Raman scattering activity. *Nanotechnology*, 22(38), 385601.

[8] Xu, X., Kim, K., Li, H., & Fan, D. L. (2012). Ordered arrays of Raman nanosensors for ultrasensitive and location predictable biochemical detection. *Advanced Materials*, 24(40), 5457-5463.

[9] Jeanmaire, D. L., & Van Duyne, R. P. (1977). Surface Raman spectroelectrochemistry: Part I. Heterocyclic, aromatic, and aliphatic amines adsorbed on the anodized silver electrode. *Journal of Electroanalytical Chemistry and Interfacial Electrochemistry*, 84(1), 1-20.

[10] Albrecht, M. G., & Creighton, J. A. (1977). Anomalously intense Raman spectra of pyridine at a silver electrode. *Journal of the american chemical society*, 99(15), 5215-5217.

[11] Le Ru, E., & Etchegoin, P. (2008). Principles of Surface-Enhanced Raman Spectroscopy: and related plasmonic effects. *Elsevier*.

[12] Stiles, P. L., Dieringer, J. A., Shah, N. C., & Van Duyne, R. P. (2008). Surface-enhanced Raman spectroscopy. *Annu. Rev. Anal. Chem.*, 1, 601-626.

[13] Albrecht, M. G., & Creighton, J. A. (1978). Intense Raman spectra at a roughened silver electrode. *Electrochimica acta*, 23(10), 1103-1105.

[14] Cao, P. G., Yao, J. L., Ren, B., Mao, B. W., Gu, R. A., & Tian, Z. Q.

(2000). Surface-enhanced Raman scattering from bare Fe electrode surfaces. *Chemical Physics Letters*, 316(1), 1-5.

[15] Vigderman, L., & Zubarev, E. R. (2012). Starfruit-shaped gold nanorods and nanowires: synthesis and SERS characterization. *Langmuir*, 28(24), 9034-9040.

[16] Theiss, J., Pavaskar, P., Echternach, P. M., Muller, R. E., & Cronin, S. B. (2010). Plasmonic nanoparticle arrays with nanometer separation for high-performance SERS substrates. *Nano letters*, 10(8), 2749-2754.

[17] Novak, J. P., & Feldheim, D. L. (2000). Assembly of phenylacetylene-bridged silver and gold nanoparticle arrays. *Journal of the American Chemical Society*, 122(16), 3979-3980.

[18] Wang, X., Li, G., Chen, T., Yang, M., Zhang, Z., Wu, T., & Chen, H. (2008). Polymer-encapsulated gold-nanoparticle dimers: facile preparation and catalytical application in guided growth of dimeric ZnO-nanowires. *Nano letters*, 8(9), 2643-2647.

[19] Kühler, P., Roller, E. M., Schreiber, R., Liedl, T., Lohmüller, T., & Feldmann, J. (2014). Plasmonic DNA-origami nanoantennas for surface-enhanced Raman spectroscopy. *Nano letters*, 14(5), 2914-2919.

[20] Li, W., Camargo, P. H., Lu, X., & Xia, Y. (2008). Dimers of silver nanospheres: facile synthesis and their use as hot spots for surface-enhanced Raman scattering. *Nano letters*, 9(1), 485-490.

[21] Wu, W., Hu, M., Ou, F. S., Li, Z., & Williams, R. S. (2010). Cones fabricated by 3D nanoimprint lithography for highly sensitive surface enhancedRaman spectroscopy. *Nanotechnology*, 21(25), 255502.

[22] Jiang, Y., Wu, X. J., Li, Q., Li, J., & Xu, D. (2011). Facile synthesis of gold nanoflowers with high surface-enhanced Raman scattering activity. *Nanotechnology*, 22(38), 385601.

[23] Perney, N. M., Baumberg, J. J., Zoorob, M. E., Charlton, M. D., Mahnkopf, S., & Netti, C. M. (2006). Tuning localized plasmons in nanostructured substrates for surface-enhanced Raman scattering. *Optics express*, 14(2), 847-857.

[24] Wang, C., Peng, S., Chan, R., & Sun, S. (2009). Synthesis of AuAg Alloy Nanoparticles from Core/Shell-Structured Ag/Au. *Small*, 5(5), 567-570.

[25] Xie, W., Herrmann, C., Kömpe, K., Haase, M., & Schlücker, S. (2011). Synthesis of bifunctional Au/Pt/Au core/shell nanoraspberries for in situ SERS monitoring of platinum-catalyzed reactions. *Journal of the American Chemical Society*, 133(48), 19302-19305.

[26] Yu, H., Chen, M., Rice, P. M., Wang, S. X., White, R. L., & Sun, S. (2005). Dumbbell-like bifunctional Au− Fe3O4 nanoparticles. *Nano letters*, 5(2), 379-382.

[27] Pradhan, M., Chowdhury, J., Sarkar, S., Sinha, A. K., & Pal, T. (2012). Hierarchical gold flower with sharp tips from controlled galvanic replacement reaction for high surface enhanced Raman scattering activity. *The Journal of Physical Chemistry C*, 116(45), 24301-24313.

[28] Li, M., Kang, J. W., Dasari, R. R., & Barman, I. (2014). Shedding Light on the Extinction-Enhancement Duality in Gold Nanostar-Enhanced Raman Spectroscopy. *Angewandte Chemie*, 126(51), 14339-14343.

[29] Novikov, S. M., Sánchez-Iglesias, A., Schmidt, M. K., Chuvilin, A., Aizpurua, J., Grzelczak, M., & Liz-Marzán, L. M. (2014). Gold spiky nanodumbbells: anisotropy in gold nanostars. *Particle & Particle Systems Characterization*, 31(1), 77-80.

[30] Yang, A., Bi, J., Yang, S., Zhang, J., Chen, A., & Liang, S. (2014). Highly surface-roughened caterpillar-like Au/Ag nanotubes for sensitive and reproducible substrates for surface enhanced Raman spectroscopy. *RSC Advances*, 4(86), 45856-45861.

[31] Sun, Y., & Xia, Y. (2002). Shape-controlled synthesis of gold and silver nanoparticles. *Science*, 298(5601), 2176-2179.

[32] Jana, N. R., Gearheart, L., & Murphy, C. J. (2001). Seed-mediated growth approach for shape-controlled synthesis of spheroidal and rod-like gold nanoparticles using a surfactant template. *Advanced Materials*, 13(18), 1389.

[33] Gao, J., Bender, C. M., & Murphy, C. J. (2003). Dependence of the gold nanorod aspect ratio on the nature of the directing surfactant in aqueous solution. *Langmuir*, 19(21), 9065-9070.

[34] Chen, J., Saeki, F., Wiley, B. J., Cang, H., Cobb, M. J., Li, Z. Y., ... & Xia, Y. (2005). Gold nanocages: bioconjugation and their potential use as optical imaging contrast agents. *Nano letters*, 5(3), 473-477.

[35] Yuan, H., Ma, W., Chen, C., Zhao, J., Liu, J., Zhu, H., & Gao, X. (2007). Shape and SPR evolution of thorny gold nanoparticles promoted by silver ions. *Chemistry of materials*, 19(7), 1592-1600.

[36] Murphy, C. J., Sau, T. K., Gole, A. M., Orendorff, C. J., Gao, J., Gou, L., ... & Li, T. (2005). Anisotropic metal nanoparticles: synthesis, assembly, and optical applications.

[37] Yuan, H., Ma, W., Chen, C., Zhu, H., Gao, X., & Zhao, J. (2011). Controllable synthesis of 3D thorny plasmonic gold nanostructures and their tunable optical properties. *The Journal of Physical Chemistry C*, 115(47), 23256-23260.

[38] Huebner, U., Schneidewind, H., Cialla, D., Weber, K., Zeisberger, M., Mattheis, R., ... & Popp, J. (2010, April). Fabrication of regular patterned SERS arrays by electron beam lithography. In SPIE Photonics Europe (pp. 771536-771536). *International Society for Optics and Photonics*.

[39] Chou, S. Y., Krauss, P. R., & Renstrom, P. J. (1996). Imprint lithography with 25-nanometer resolution. *Science*, 272(5258), 85.

[40] Wu, W., Hu, M., Ou, F. S., Li, Z., & Williams, R. S. (2010). Cones fabricated by 3D nanoimprint lithography for highly sensitive surface enhancedRaman spectroscopy. *Nanotechnology*, 21(25), 255502.

[41] Hao, F., Nehl, C. L., Hafner, J. H., & Nordlander, P. (2007). Plasmon resonances of a gold nanostar. *Nano letters*, 7(3), 729-732.

[42] Sau, T. K., & Murphy, C. J. (2004). Room temperature, high-yield synthesis of multiple shapes of gold nanoparticles in aqueous solution. *Journal of the American Chemical Society*, 126(28), 8648-8649.

[43] Xie, J., Zhang, Q., Lee, J. Y., & Wang, D. I. (2008). The synthesis of SERS-active gold nanoflower tags for in vivo applications. *ACS Nano*, 2(12), 2473-2480.

[44] Wu, H. L., Chen, C. H., & Huang, M. H. (2008). Seed-mediated synthesis of branched gold nanocrystals derived from the side growth of pentagonal bipyramids and the formation of gold nanostars. *Chemistry of Materials*, 21(1), 110-114.

[45] Anderson, B. D., & Tracy, J. B. (2014). Nanoparticle conversion chemistry: Kirkendall effect, galvanic exchange, and anion exchange. *Nanoscale*, 6(21), 12195-12216.

[46] Bardhan, M., Satpati, B., Ghosh, T., & Senapati, D. (2014). Synergistically controlled nano-templated growth of tunable gold bud-to-blossom nanostructures: a pragmatic growth mechanism. *Journal of Materials Chemistry C*, 2(19), 3795-3804.

[47] Jiang, Y., Wu, X. J., Li, Q., Li, J., & Xu, D. (2011). Facile synthesis of gold nanoflowers with high surface-enhanced Raman scattering activity. *Nanotechnology*, 22(38), 385601.

[48] Guerrero-Martínez, A., Barbosa, S., Pastoriza-Santos, I., & Liz-Marzán, L. M. (2011). Nanostars shine bright for you: colloidal synthesis, properties and applications of branched metallic nanoparticles. *Current Opinion in Colloid & Interface Science*, 16(2), 118-127.

[49] Yu, Y. Y., Chang, S. S., Lee, C. L., & Wang, C. C. (1997). Gold nanorods: electrochemical synthesis and optical properties. *The Journal of Physical Chemistry B*, 101(34), 6661-6664.

[50] Wang, W., Dahl, M., & Yin, Y. (2012). Hollow nanocrystals through the nanoscale Kirkendall effect. *Chemistry of Materials*, 25(8), 1179-1189.

[51] Prabhakaran, M. P., Vatankhah, E., Kai, D., & Ramakrishna, S. (2015). Methods for Nano/Micropatterning of Substrates: Toward Stem Cells Differentiation. *International Journal of Polymeric Materials and Polymeric Biomaterials*, 64(7), 338-353.